



Proposal

Development of a New Detector Technology for Fiber Sampling Calorimeters for EIC and STAR

H. Z. Huang, G. Igo, S. Trentalange, O. Tsai
University of California at Los Angeles

C. Gagliardi

Texas A&M University

S. Heppelmann

Pennsylvania State University

8/1/2009, latest update 03/31/2011

We propose to develop a new technology based on tungsten powder and fiber readout to construct sampling electromagnetic and hadronic calorimeters. The proposed technique aims at building compact and fine grained devices with good energy resolution, hermeticity, homogeneity, timing and position resolution. The proposed detector technology is very simple, cost effective and flexible enough to optimize in configurations demanded by different physics requirements. This technology is well-suited to take advantage of new developments in photo-detectors (APD, SiPMT). Such electromagnetic and hadronic calorimeters can be used for photon measurements and recoil jets at EIC and for electron and hadron energy measurements in STAR future upgrades or eSTAR configurations.

Introduction

We propose to build sampling calorimeters with active elements consisting of fibers. The fibers can be scintillating, quartz, non-scintillating optical fibers or any combination of these depending on the device being built. A combination of different fibers as active elements in the detectors can be selectively used to read out scintillation and/or Cherenkov light produced by showering particles. As the absorber (radiator) we will use tungsten powder for all devices being proposed for construction. Utilization of tungsten powder as an absorber opens unique ways to construct fiber calorimeters. Common problems that were encountered in previous fiber calorimeters can be potentially eliminated or reduced with our technique. Fig. 1 presents cross sectional snapshots of an excellent fiber calorimeter used in the past (H1) and of the prototype discussed in this proposal.

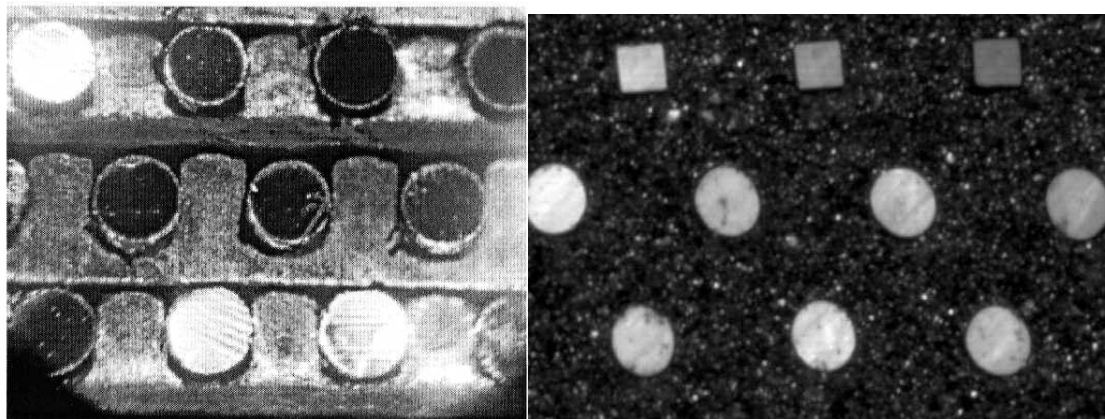


Fig. 1. Fiber/absorber structure of typical ScFi calorimeters (H1 calorimeter) (left); fibers 0.5 mm in diameter, fiber spacing 0.9 mm. (right) Fiber/tungsten absorber of a UCLA mechanical prototype, upper row: square fibers 0.25 mm x 0.25mm, lower rows: round fiber 0.33 mm diameter, spacing 0.88 mm.

Spaghetti fiber sampling calorimeter technology has unique features and characteristics. We note below a section from the CERN-95-02 Yellow Report “Scintillating-fiber Calorimetry” [1].

“11. Conclusions

Since the moment when fiber calorimeters were first introduced, less than ten years ago, they have rapidly gained a reputation as one of the most attractive detectors available for modern particle physics experiments. This reputation is due to a combination of the following factors:

1. Fiber calorimeters are among the fastest particle detectors available today. Given the extremely high luminosities, and the correspondingly small time intervals between events, needed to extract envisaged new physics phenomena, this is an important feature.
2. The excellent resolution in energy and position measurements that can be achieved with a very compact instrument is a property characteristic of fiber calorimeters. As pointed out in section 10.4 this resolution is achieved through very frequent shower sampling and in this way, e.m. energy resolutions of the order of $6\%/VE$ can be achieved with sampling fractions as low as 10% (fig. 104). Depending on the absorber material that is used, the effective density of such a detector will be in the range of 5-10 g/cm, with an effective radiation length of 1 cm or less and Molière radius of 2 cm or less. Given the high cost of radial space in 4π experiments and the high particle density, which makes pencil-like showers very desirable, these are invaluable detector properties.
3. The fiber structure of the active calorimeter material has solved the hermeticity problem inherent to all scintillator-based calorimeters used in the past. Since the fibers both generate the light and transport it to the outside world, no separate wavelength-shifting devices, with corresponding non-hermeticity introduced by these, are needed. ...
4. The high light yield makes it possible to achieve energy resolution compatible with the ones obtained with the homogeneous calorimeters. The KLOE Collaboration (section 8.3) found that the contribution of the photoelectron statistics to the energy resolution of their calorimeter was only $2\%/VE$. The 1500 photoelectrons per GeV found by RD1 for their calorimeter [67], which had a sampling fraction of less than 5% for e.m. showers, limit the contribution of photon statistics to the resolution to only $2.6\%/VE$. Combined with the extraordinarily low noise levels achieved with the PM readout, this high light yield makes dynamic range of fiber calorimeters very large (at least 6 orders of magnitude). As a result, small energy deposits, for example in the tails of hadronic showers or from traversing muons, can be accurately measured.
5. Last but not least, fibre calorimeters are cheap devices. Depending on the complexity of the readout, high-resolution e.m. fibre calorimeters are up to an order of magnitude cheaper than crystal calorimeters (BGO, BaF₂, CeF₃, PbWO₄, HfF₄, etc.).

Some of the advantages listed above are especially important for the detection of electromagnetic showers. For example, the energy resolution of hadron calorimeters is also determined by factors other than sampling fluctuations and, therefore, does not benefit from choosing fibers to the same extent as e.m. calorimeters. Also, hermeticity requirements are usually less stringent in the hadronic section of the calorimeters system. Obviously, as illustrated by SPACAL, one can also make excellent hadron calorimeters with the scintillating fibers as active elements, but the advantages over other techniques are somewhat less striking than in the case of e.m. shower detectors.”

Although development of new EM calorimeters based on fiber technology has mainly halted (GlueX at JLAB follows KLOE design), the development of fiber hadronic calorimeters has continued, for example, with the R&D DREAM (Dual-REAdout Module) project. The term “Dual-REAdout” refers to readout of scintillation and Cherenkov light at the same time from different fibers (sc. and non-sc.) in a hadronic calorimeter. This allows the measurement of the electromagnetic fraction in the hadronic shower on an event-by-event basis. The authors of the DREAM project argue that with this approach the theoretical resolution limit of $\sim 15\%/VE$ for hadronic showers seems to be within reach [2]. The results of the DREAM project were presented at the XIth International Conference on Calorimetry in High Energy Physics (Perugia, Italy, 2004) and represented a major advancement in calorimetry technology.

To summarize this section we present two tables with the available EM and hadronic resolution data for fiber calorimeters. The following expressions were used for energy resolutions:

$$\frac{\sigma}{E} = \frac{a}{\sqrt{E}} + C \quad (1)$$

$$\left(\frac{\sigma}{E}\right)^2 = \left(\frac{a}{\sqrt{E}}\right)^2 + (C)^2 \quad (2)$$

Detector	Composition	Energy Range (GeV)	a,c eq. (1)	a,c eq.(2)	Comments
Burmeister <i>et al.</i>	Pb 1:1	0.04-1	9.8, -		Fibers $\phi = 1\text{mm}$, Ribbons \perp to the beam.
JETSET	Pb 35:50	0.3-1.5	6.3, -		$\phi = 1\text{mm}$, glue 15%
SPACAL	Pb 4:1	5-150	12.9,1.23	15.7, 1.99	$\phi = 1\text{mm}$
RD1	Pb 4:1	10-150	9.2, 0.63	10.9, 1.11	$\phi = 0.5\text{mm}$
RD1	Pb 1.8:1	10-150	8.0, 0.35	8.9, 0.72	$\phi = 1\text{mm}$
RD25	Pb 4:1	2-50	15.0, 0.5	16.0, 1.4	$\phi = 1\text{mm}$
RD25	Pb 4:1	2-80	14.4, 0.17	14.7, 0.68	$\phi = 1\text{mm}$
LEP-5	Alloy 4:1	2-8	16.0, 1.6		$\phi = 1\text{mm}$
KLOE	Pb 35:50	0.02-0.08	4.8, -		$\phi = 1\text{mm}$, glue 15%, fibers \perp to the beam.
CHORUS	Pb 4:1	2.5-10	13.9, 0.1	14.1, 0.7	$\phi = 1\text{mm}$, fibers \perp to the beam.
H1	Pb 2.27:1	2-60		7.1, 1	$\phi = 0.5\text{mm}$

Table 1. Electromagnetic resolution of fiber calorimeters. Data taken from [1] and [3].

The total hadronic resolution of the two best calorimeters (approximately compensated) and the various factors contributing to it are listed in the table below (where σ_p , σ_s , σ_i are the fluctuations in the number of signal quanta, sampling fluctuations and intrinsic fluctuations, respectively.)

	ZEUS ²³⁸ U	ZEUS Pb	SPACAL
σ_p	6%/VE	10%/VE	5%/VE
σ_s	31%/VE	42%/VE	27%/VE
σ_i	19%/VE	11%/VE	11%VE
σ_h	37%/VE	44%/VE	30%/VE

Table 2. Hadronic energy resolution of different calorimeters. Data taken from [4,5,6,7]

In all three detectors, the hadronic resolution is dominated by sampling fluctuations. This is a direct consequence of compensation ($e/h = 1$), which requires small sampling fractions, for example, 2.3% for lead/plastic detectors and 5.1% for uranium/plastic devices. Our technique aims to reduce the sampling fluctuations in calorimeters by increasing the sampling frequency to a level which was considered impractical for traditional methods of construction of fiber calorimeters.

The remainder of the proposal is organized as follows. First, in Figure 2 we present a possible road map for our proposed R&D. In the electromagnetic section (Section 2) we will briefly summarize past developments in fiber calorimetry technology, including our own results. In the hadronic section (Section 3) we will discuss an application of our technique for compensated hadronic calorimeters.

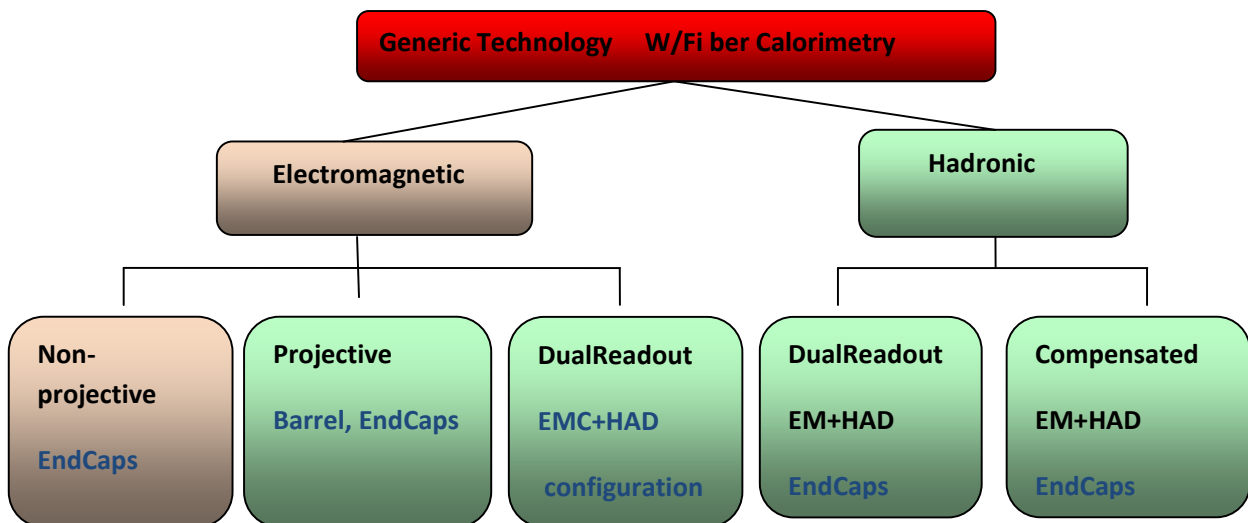


Fig 2. Possible R&D directions and applications for EIC detector(s).

The presentation in Figure 2 reflects both R&D directions and possible applications at EIC. For example, the most basic and simplest to construct would be an electromagnetic calorimeter with non-projective geometry which may be used in the endcap regions. Successful tests of a prototype would be a proof of principle which is our main objective for the first year of R&D.

Electromagnetic fiber calorimeters R&D

The precision of sampling calorimetric measurements is determined and limited by fluctuations. In reasonably designed detectors, the precision is dominated by the sampling fluctuations. Sampling fluctuations are determined by the amount of active material(s) in the detector (sampling fraction) and the sampling frequency (thickness of active layers). In calorimeters with non-gaseous active media the energy resolution is well described by [8]:

$$\frac{\sigma}{E} = \frac{2.7\%}{\sqrt{E}} * \sqrt{\frac{d}{F_s}} \quad (3)$$

where d is the thickness of the active elements (e.g., diameter of the fibers in mm) and F_s is the sampling fraction for mips.

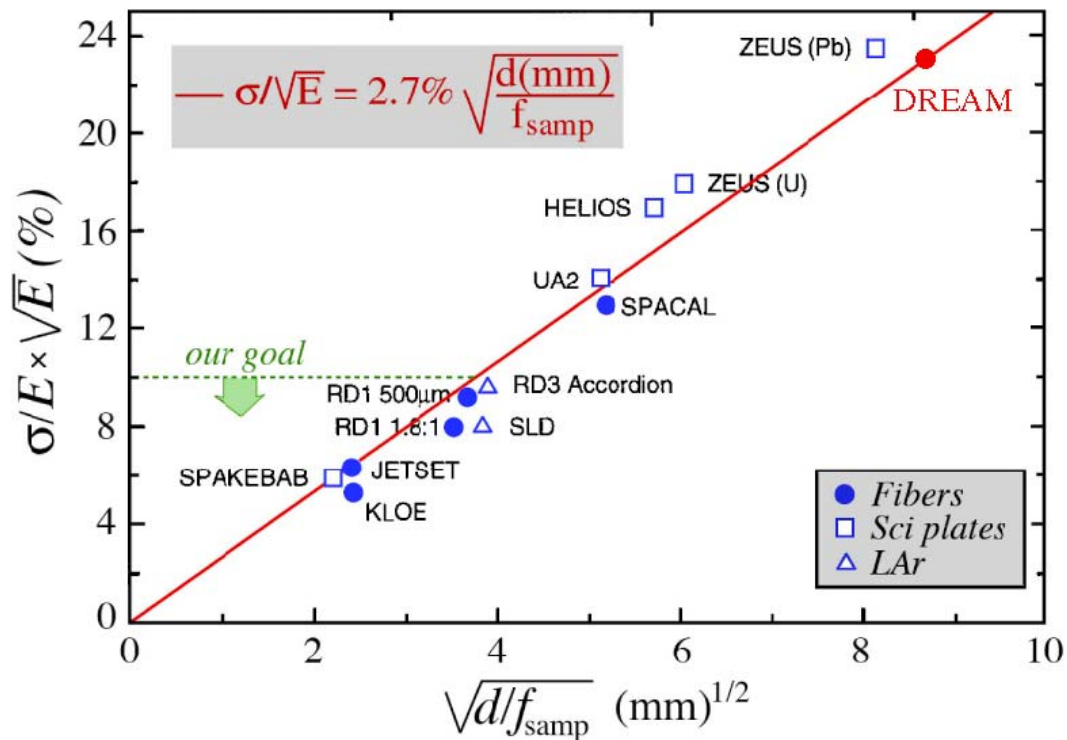


Fig. 3. Electromagnetic energy resolution as a function of sampling fraction, for various non-gaseous calorimeters. This figure is taken from R. Wigmans presentation at CALOR2010, see also ref. [1].

Compact and compensated calorimeters require small F_s . The use of fibers as an active media in calorimeters allows us to meet this requirement. As discussed in [1], improvement of the EM energy resolution through an increased sampling frequency has its limits. It is not practical to increase the sampling frequency significantly due to the fact that working with increasingly thinner fibers and

absorber layers rapidly becomes very cumbersome. This is probably one of the reasons that no one has used fibers thinner than 0.5 mm in diameter in full scale detectors. We will demonstrate that our technique is practically free from this limitation.

R&D projects in the past have employed various ways to construct calorimeter prototypes, i.e. simple piling with gluing, casting or brazing the absorber matrix, with the fiber being inserted into channels afterward. Independent of which of these techniques was used, their common weakness was an extremely low level of automation in the assembly process. Essentially every fiber or absorber layer had to be handled manually. This contributed to higher costs for fiber calorimeters compared to scintillation plate detectors. This also limited the sampling frequency because thinner absorber layers and thinner fibers become difficult to handle. The other common characteristic of previous mechanical designs of fiber calorimeters is the placement of fibers inside the absorber volume. To our knowledge, all detectors have had fibers placed in straight lines, parallel to each other in order to keep the sampling frequency within the tower volume constant. This is a direct consequence of the construction of the absorber matrix from machined, rolled or extruded sheets.

A succinct description of our proposed technology is the following: We form a matrix of fibers and then the absorber is poured into this matrix. This differs from previous techniques, in that individual elements of the calorimeter do not need to be handled separately.

Two prototypes were constructed by UCLA group in 2003 and 2004 using tungsten powder as an absorber. The motivation at that time was purely conceptual, namely, to develop a technology which could be used in compact detectors. Compact detectors are feasible due to the remarkable progress made in micro-pattern detectors.

The key element in our technique is the utilization of tungsten powder as an absorber. We Tungsten powder has: particle size distribution 90% between 40 and 150 microns, bulk density 18.5 g/cm^3 , tap density 11.25 g/cm^3 . The chemical composition is: W > 99.3%, Fe < 0.05%, Ni < 0.05%, O₂ < 0.5%, others (Co, Cr, Mo, Cu) < 0.5%. Tungsten powder also has very good fluidity, an important property in our applications.

Our first prototype had 16 towers. The towers were composed of W powder and square 0.25 mm x 0.25 mm BCF-12 scintillation fibers. There were 496 fibers per tower with 1 mm spacing between the fibers center-to-center, in a staggered pattern. The active volume was $22 \times 22 \times 120 \text{ mm}^3$. The final density for different towers differed slightly, but for most, were about 10.25 g/cm^3 . Slight variations in final density were due to different methods used to pour W powder into the fiber matrix. Taking the effective radius of the fibers as 0.28 mm and a sampling fraction for mips of 1.2%, the stochastic term for energy resolution according to equation (3) should be close to 13%. A photograph of one of the towers is presented in Fig. 4.



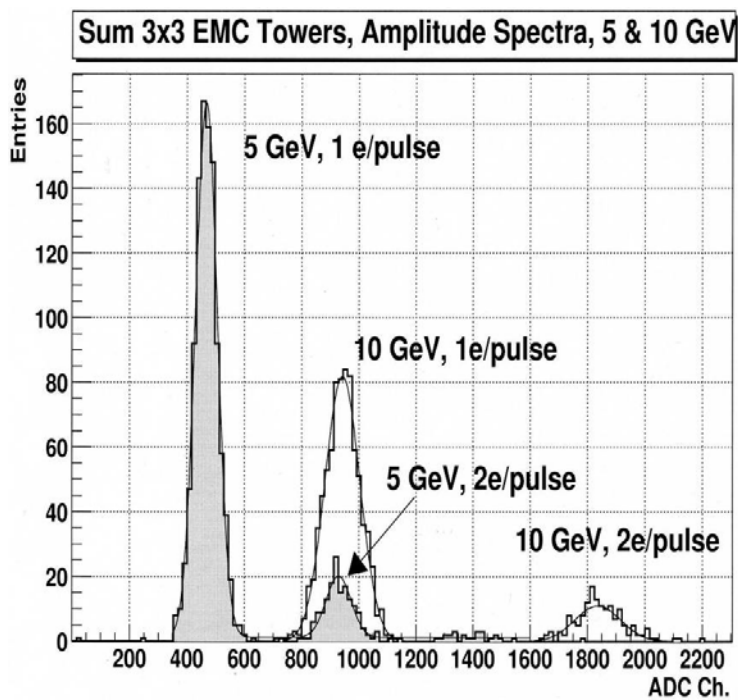
Fig. 4. Photograph of a single tower of our first prototype with internal structure drawn on the wall of the brass container (scale is in cm). On the right is a view from the photodetector side (not to scale).

The mechanical structure of this prototype required a thin walled (thickness 125 micron) brass container to keep powder and fibers in place. To assemble it, fibers were cut to ~ 15 cm length. One end of the fiber was slightly melted to form a small drop which worked as a stopper to prevent the fibers from slipping through the openings in the mesh. A stack of two meshes was populated with fibers by undergraduate students. The lower mesh was fixed at the end of the brass container and this end of assembly was dipped into optical epoxy. Once the epoxy cured, tungsten powder was poured into the container from the top and at the same time the second mesh was pulled to the top of the container. Powder flowed into the container through the openings between the walls of mesh holes and fibers and filled the space from the bottom of the container, at the same time fixing fibers in place. During the filling process, the whole assembly sat on a vibrating platform. A delrin cap with openings for the fibers was used to close the container and the fibers were epoxied to the cap. The small diameter of the fibers makes them very flexible, with very little space needed to form a bundle of fibers at the end of the tower as seen in Fig. 4. The final steps was to machine both ends of the container and to glue a front face mirror (black block at position 0 cm in Fig. 4) onto the front and a light guide onto the back of the tower. Using this technique, very compact assemblies could be made, but, as we learned during a later test run, this method had significant flaws requiring a change in the technique.

The first prototype matrix 4x4 towers was tested at the SLAC FFTB test line in 2003. The photodetectors we used were Hamamatsu R7400U mesh photomultipliers with additional external amplifiers and S8664-55 APDs operated at a gain of 50. A photograph of the test setup is presented in Fig. 5.



Fig. 5. Beam test setup at the SLAC FFTB line. A coincidence between scintillation counters Sc1 and Sc2 provided the trigger. Two small MWPCs provided XY coordinates to determine the impact point. The EMC was positioned on a 2D moveable platform.



During calibration of the individual towers, we found that the observed energy resolution was not what we expected to see. The most striking observation was the variation by a factor of two of the energy sum of a 3x3 tower cluster during the transversal scan of the matrix. Most of the 36 hours beam time allotted for the test was spent for different type of scans of the matrix both in the transverse and longitudinal directions. The results are summarized in Figure 6. The best energy resolution for a single tower with impact point at the tower center was determined to be $17\%/VE$.

Fig. 6 Energy distribution for 3x3 sum of amplitudes during SLAC test run for Prototype 1.

The origins of large transverse non-uniformities were understood. The major contributing factors were dead layers near the tower edges and missing fibers in the tower corners (instead of 500 fibers we were left with 496 as four fibers, one in each corner of the tower were removed to allow for strings to pull the second mesh during filling). The non-uniformities observed during the longitudinal scans of the towers ($\pm 10\%$ maximum along the tower) were not well understood. The largest variations of response were observed for points located from 4 to 9 X_0 radiation lengths along the towers. One plausible explanation was that during packing process and recompression during stacking the array, the brass container might have undergone a slight distortion in the middle which led to a decreased sampling fraction in this region. There is also an indication that the cladding light might not be properly suppressed. Another factor that might have contributed to the non-uniform response was that the light guide at the end of the tower was not optimized prior to the test run. As we realized post factum, problems with non-uniformities were observed by other groups and were described in ref [1]. Dense calorimeters will require very strict mechanical tolerances and a very uniform internal structure to achieve uniform response across the detector. A good example in this respect is the H1 electromagnetic calorimeter where tight mechanical tolerances were required during sub-module construction and final assembly of the detector.

To solve the problems with our first prototype we developed another method of combining powder and fibers. First we learned how to infuse optical epoxy into packed powder. A vacuum-assist method allows infusion of BC600 epoxy to a depth of 20 mm within 20 minutes. Epoxy has to be infused after packing because only dry powder has good fluidity. A few mechanical samples with a density of $\sim 10.55 \pm 0.05 \text{ g/cm}^3$ were examined for uniformity. Local density variations were found to be within 2%. To

keep sampling frequency uniform along and across the tower we added additional intermediate meshes. These additional meshes allows arrangement of fibers in an accordion configuration, thus we got a “spacordion” structure. Since the whole assembly becomes rigid and stable there is no need for any type of external container. This eliminated dead material in the tower assembly. A single molding form was used to produce all subassembly units, which assured good mechanical tolerances and uniform sampling frequency between the towers. This time we used fibers with a diameter of 0.33 mm to match the openings in available standard perforated meshes. The distance between the fiber centers was 0.88 mm. Photographs of the mechanical prototype structures (with the square fibers left over from the first prototype) are shown in Fig. 7.

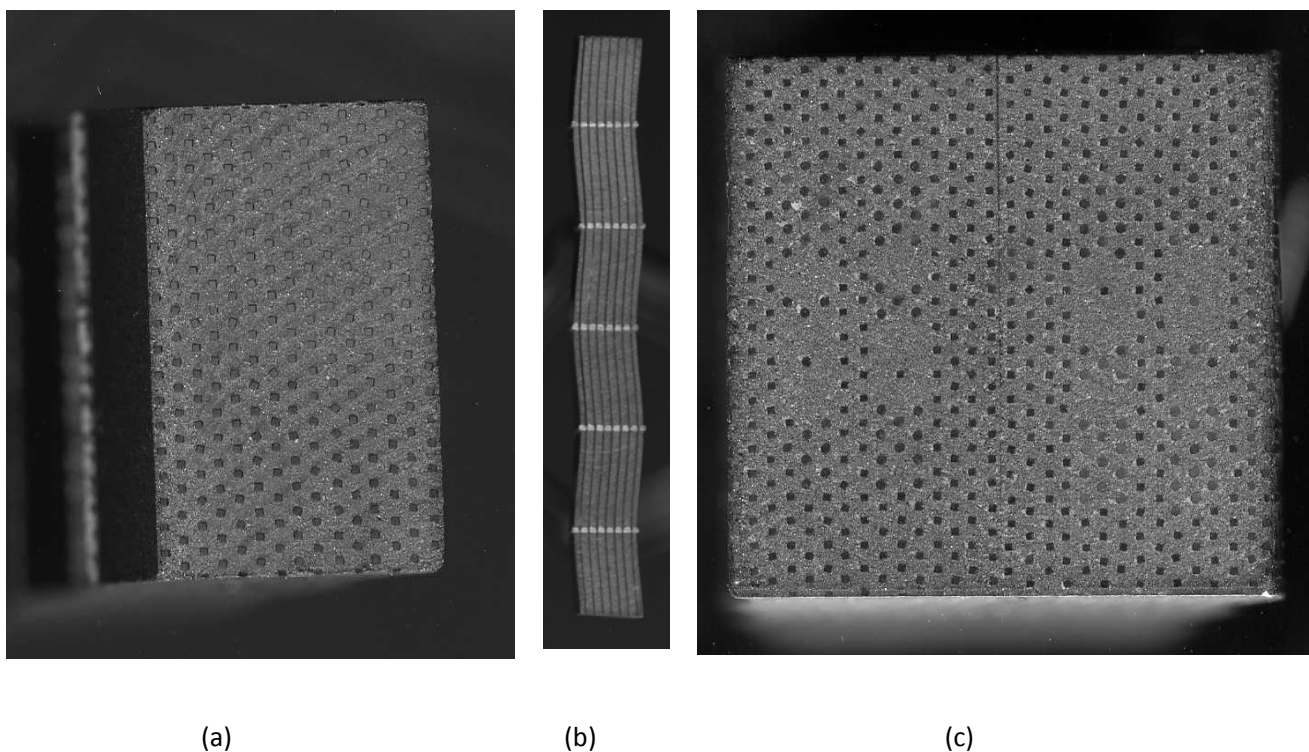


Fig. 7. Front (a) and top (b) view of the cross sections of the mechanical subassembly prototype. The distance between fiber centers is 0.88 mm. The fibers are placed in an accordion geometry. (c) shows cross section of mechanical prototype glued from two subassemblies. Good sampling uniformity is preserved right to the edges of the towers. This should solve problems with non-uniformities we experienced with our first device.

For the second prototype, every tower was glued from two sub-assemblies which have the structure shown in Fig. 7(a,b). The reason for this is the stiffness of 345 fibers in a single sub-assembly unit, e.g. it was difficult to arrange 670 fibers in an accordion shape at the same time. We believe that there multiple advantages for arranging fibers in an accordion type structure compared to the standard technique. First, all angular dependences should be significantly reduced. In particular, there is no way that a showering particle can cross the detector along the fiber (channeling effect for fiber calorimeters). Second, for a given number of fibers, both the effective sampling frequency and sampling fraction are

increased. Third, the number of fibers which contribute to the signal is increased, thus resolution degradation due to non-uniformities in the response of a single fiber also should be reduced. With conventional construction techniques for fiber calorimeters, to create a “spacordion” structure would be almost impossible.

For our second EMC prototype we constructed a 3x4 matrix with the structure of towers as shown above. The size of this prototype was small, in order to learn how well this technique would work. Strict constraints on time, budget and manpower did not allow us to construct a larger detector. The final assembly unit, before the PMT block was attached, is shown in Fig. 8.

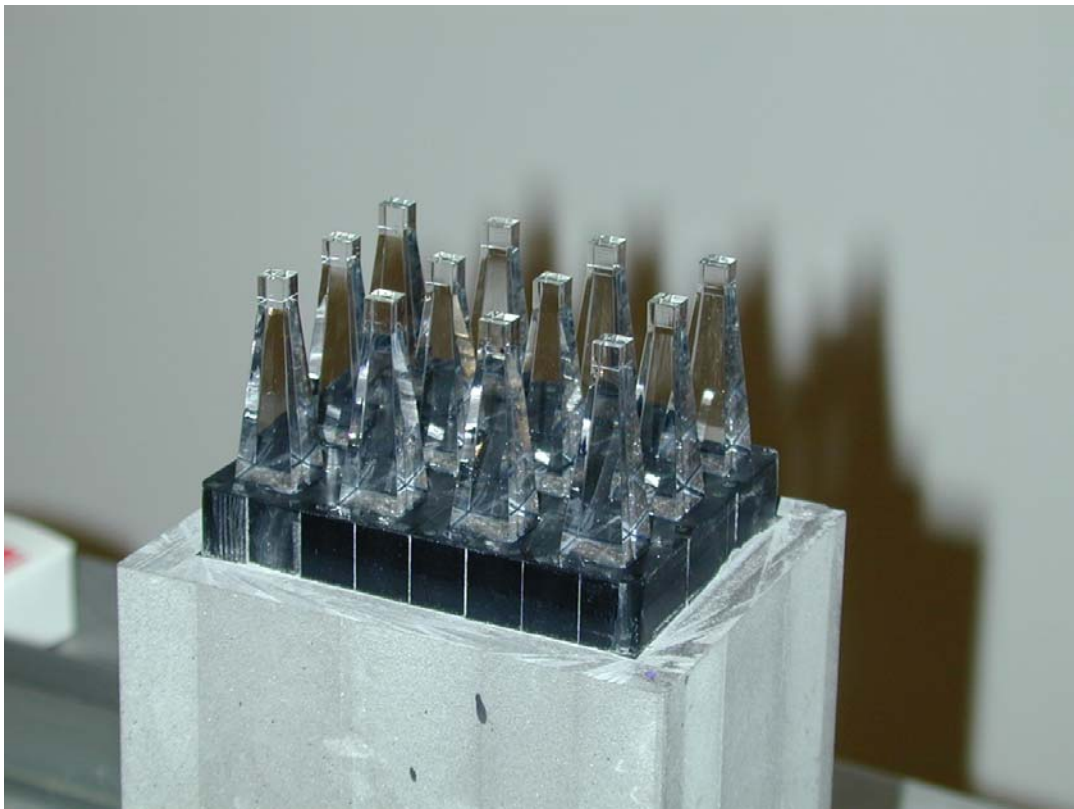


Fig. 8. Photograph of the final assembly. Black Delrin blocks where fibers were bundled have the size of an active area. The external container (the gray material), is a mixture of W powder and epoxy it minimizes edge effects for active towers.

Quite long and complicated light guides were required to achieve good uniformity of response across the surface of the tower with R5700U PMT readout. The size of the light guides at the end was chosen to be $4.9 \times 4.9 \text{ mm}^2$ to allow readout with S8664-55 APDs as a second option. This reduced the cross section of the fiber bundle by about a factor of three.

This second prototype was scheduled for a test run at SLAC in the fall of 2004. The test run was unfortunately delayed, and then SLAC was shut down due to an accident at the accelerator complex. We have not had an opportunity to test this prototype with a beam. This method of building fiber calorimeters has yet to be tested.

To obtain a “proof of principle”, we now propose to build a larger prototype using techniques developed for our second device and perform a beam test for the prototypes. We will use the same structures (fibers/meshes) and the expected energy resolution should be close to $10\%/VE$. The radiation length and Molière radius will be about 0.7 cm and 1.8 cm. Ideally, we would like to use square fibers. There are three reasons why: better trapping efficiency for light, larger surface area for the same sampling fraction compared with cylindrical fibers and a smaller output surface area because they pack much better. However, there are no available off-the-shelf perforated meshes with the desired dimensions. If we find appropriate meshes then we will use square fibers. We propose to expand the transverse tower size for this new prototype to about $2.8 \times 2.8 \text{ cm}^2$. The length of the towers will be $20X_0$. We also would like to change slightly the method we used to construct the towers. For this third prototype we will build towers from four sub-tower units. We believe that a matrix of 4×4 towers would allow us to determine the efficiency of this technique with good confidence. We plan to use conventional PMT readout in the first year of the R&D.

If this technique works, (e.g. energy resolution, linearity and uniformity measured in the test run are good), then there are a few additional factors that we will investigate with this third prototype. The objectives are:

1. Investigate mechanical stability of the assembly; in particular, investigate how the parameters (optical, mechanical) of the towers will change under mechanical load.
2. Investigate radiation hardness of the device, e.g. look at effects of radiation damage on scintillation fibers. Although good data exists in the literature [10] and general trends are known, in each case such studies have to be performed for the unique components of individual detectors. For us it would mean that after irradiation we would like to test this prototype with the beam one more time.
3. Investigate new readout techniques (using APDs or SiPMTs).

It is likely that these efforts will be carried out in the second phase of this R&D project.

Hadronic Fiber Calorimeter R&D

If we find out that our technique works well for electromagnetic calorimeters we then will continue our R&D effort for hadron calorimeters. Applicability for both compensated and non-compensated dual readout devices can be investigated.

Advocates for fiber calorimetry technology like to compare the performance of the SPACAL calorimeter with the expected performance of two new detectors at LHC as shown below in Fig. 9 (from [11]). The point of showing the results this way is to illustrate that, until recently almost all calorimeter systems represent a compromise if one wants to measure both EM and hadronic showers. For example,

the ZEUS collaboration operated a very-high-resolution hadron calorimeter, but paid a price in the form of rather mediocre performance for EM shower detection (18%/VE). This was a direct consequence of requiring compensation, which demands a small sampling fraction, which in turn leads to large sampling fluctuations. On the other hand, if one focuses on excellent EM resolution, one pays a heavy price when it comes to hadronic shower detection.

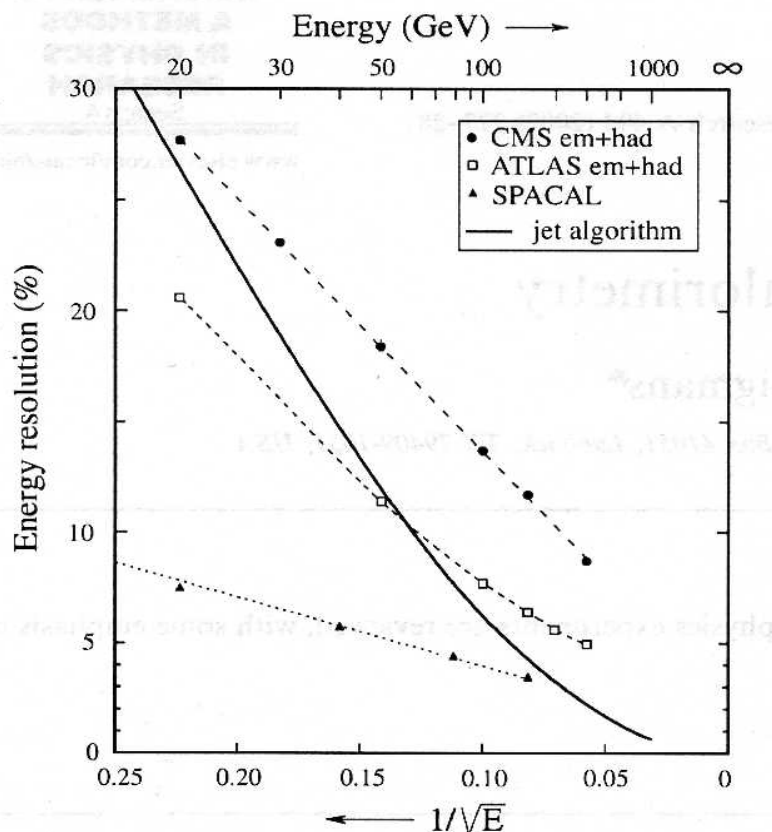


Fig. 9. The hadronic energy resolution of three calorimeter systems and the contribution of a jet-defining cone with $R=0.3$ to the jet energy resolution, as a function of energy.

As the author of [11] pointed out, once the choice is made for a crystal EM section (with a single readout technique), it essentially does not matter what you install behind it. The hadronic energy resolution will be poor. It will be completely determined by fluctuations in the energy sharing between the EM and hadronic calorimeter sections, which have very different e/h values. Even the most sophisticated compensating hadronic section cannot alter this conclusion.

Non-compensated calorimeters are intrinsically non-linear for hadrons, because of the energy dependence of the average EM shower fraction f_{em} . In the case of the CMS system, the large e/h value for crystals has the effect of deterioration of the hadronic signal linearity compared to stand-alone HCAL performance. Another adverse effect concerns the shape of the hadronic response function. Non-gaussian fluctuations in f_{em} tend to make the line shape asymmetric, which may have serious

consequences for triggering. Calibration of non-compensated devices can be very tricky. As shown in [13] response of the calorimeter for high energy protons and pions may differ as much as 15%. Although for a known particle type one can make corrections, in the case of jets where the particle mix is unknown these corrections cannot be performed.

The dual-readout technique potentially solves all the problems mentioned above. The proof of principle is presented in [12] where a calorimeter system with a dual readout EM section made of BGO crystals followed by a dual readout DREAM hadronic section provide excellent resolution for both EM and hadronic showers.

The TESLA project [14] used a different approach to achieve excellent energy resolution for jets, usually referred to as the energy flow method (STAR is doing something similar for jet reconstruction using a TPC and barrel EMC with known limitations). The charge fragments of jets can be measured more precisely with the tracker than with the calorimeter. However, calorimeter information is still needed to account for contributions from neutral particles, mainly photons from π^0 , but also K_s^0 and neutrons. To do that properly, a very high-granularity calorimeter will be required. A high granularity allows recognition and elimination of all contributions from charge particles to the overall calorimeter signal. The remaining signal then can be assigned to the neutral components of the jet. For illustration Fig. 10 shows a SPACAL event display for a 150 GeV pion interacting with a thin target placed 1.5 m upstream.

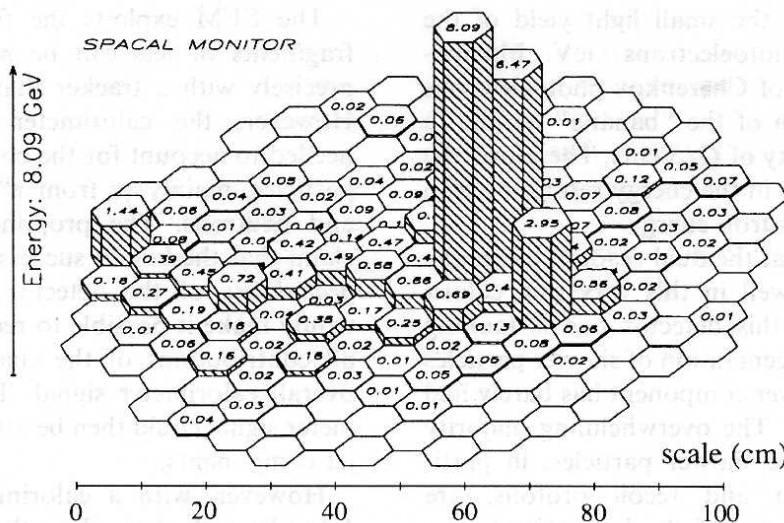


Fig. 10. A SPACAL event displays the reaction products from a 150 GeV pion interacted in an upstream target. The numbers denote the energy in (GeV) deposited in the individual calorimeter cells [15].

SPACAL was a very fine-grained calorimeter with the effective radius for each cell of $0.19 \lambda_{\text{int}}$ ($2.0 R_M$). Our proposed effective cell size will be comparable to SPACAL. Smaller granularity will not help since the size of the cell is already at the level when even electromagnetic showers will be spread among a few of them. For this reason, as proponents of SPACAL point out [11], the calorimeter system needs other

qualities besides high granularity. In particular, it needs a good hadron energy resolution in order to measure jet energies with good precision.

The discussion in this section (Section 3) conveys that optimization of a hadron calorimeter or combined EM + hadron calorimeter system for an experiment is a challenging task. For EIC this task is even more complicated because of the broad range of colliding species which can be potentially studied.

We would like to investigate applications of our technique to build compensated hadronic calorimeters. To do that we will propose to build a prototype with a tower size of about $3 \times 3 \text{ cm}^2$ and length of $\sim 6 \lambda_{\text{int}}$. The size of the hadronic prototype has to be significantly larger than the EM prototype, because for hadron calorimeters all sizes scale with λ_{int} . The longitudinal and radial containments $L_{95\%}$ and $R_{95\%}$ which are the required length and radius of the calorimeter for 95% hadronic energy deposition containment as given in [18] scales as:

$$L_{95\%} \approx t_{\text{max}} + 2.5 \lambda_a, \quad R_{95\%} \approx 1 \lambda_{\text{int}}, \quad (4)$$

where $t_{\text{max}} \approx 0.2 \ln[E(\text{GeV})] + 0.7$ is the shower maximum depth, and λ_a (in units of λ_{int}) describes the exponential decay of the cascade beyond t_{max} and varies with the energy as $\lambda_a = [E(\text{GeV})]^{0.13}$.

Possible Applications at EIC and in STAR and eSTAR Upgrades

Here we discuss a specific application of the proposed technique for the STAR detector. The STAR collaboration is considering an extension of research program in the forward direction with several detector upgrades. Possible physics measurements in the forward direction include jets, leading particles, Drell-Yan pairs from p+p and p+A collisions. Extension of these measurements in A+A collisions is also being considered and will require more simulations. Physics considerations for the STAR forward direction detector upgrade require good $e/h/\gamma/\pi^0$ separation. A SPACAL type detector is a leading detector choice which may meet these requirements. However, challenging space constraints, magnetic fields, availability of overhead crane access and potentially future complete redesign of the IP area, and STAR detector in the forward direction for EIC makes traditional techniques of building ScFi calorimeters difficult to use. Shown below are some possible staged transformations of the STAR detector to eSTAR on the West side.

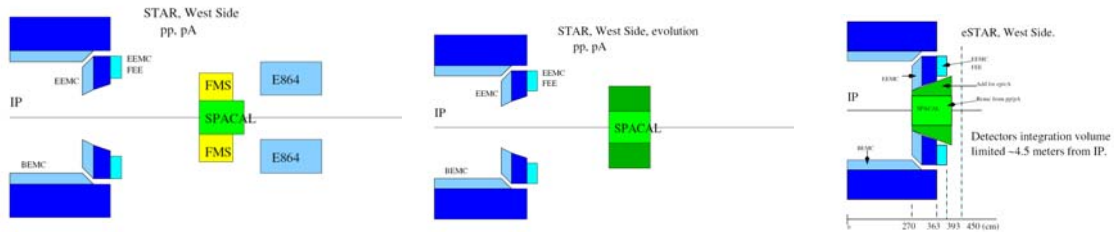


Fig. 11. Possible configuration and transformation of calorimeters on the West side of (e)STAR. Tracking would likely be installed in front of any one of these configurations, possibly utilizing GEM disks similar to those currently under construction for the STAR Forward GEM Tracker (FGT).

Preliminary investigations lead us to believe that a SPACAL type detector may be the most attractive detector choice for the proposed physics program, based on the experimental results obtained by SPACAL collaboration. The exact parameters of the SPACAL type calorimeter for STAR (eSTAR) are under investigation. One of our graduate students is running standalone GEANT4 MC to do preliminary optimization of HCAL for STAR. The construction method developed for EM calorimeter can be extended for HAD calorimeter. We will also investigate other simple techniques for detector construction. For example, the detector can be constructed with a single container holding the fiber assemblies and dry tungsten powder. The detector could be constructed in place by filling the container with fiber assemblies and tungsten powder layer by layer without using the epoxy. To reconfigure the setup for EIC, the detector will be disassembled into its components by draining the powder from the bottom. If the fiber assemblies survive this process then the fibers also can be re-used for eSTAR. R&D effort will be needed to investigate feasibility and detector performance with this construction technique.

To fully investigate method(s) of construction for hadron calorimeters we propose to continue the R&D program in Year Two, assuming the results from the Year One of this R&D will be good. However, given STAR's time constraint for the forward direction upgrades, it will be necessary to start R&D for the hadron calorimeter in the first year with a small prototype. Thus, we propose to build a small prototype of the combined EM+Hcal calorimeter in Year One and test it as an electromagnetic calorimeter only (because of small transverse size of the detector, the length of the detector will be about 6 interaction length). We will test this prototype and the "spacordion" EM type detector described earlier during the same test run in the first year of R&D. If successful, we will propose to extend the size of the Hcal prototype in the second stage of this R&D effort and to test it as a hadronic calorimeter, with potentially new readout using APDs or SiPMTs.

Summary

In phase one of the proposed R&D project we plan to obtain "proof of principle" with the construction and beam test of a small EM prototype consisted of 16 towers, build with the "spacordion" technology. At the same time we would like to investigate alternative methods to construct compensated, highly granulated hadronic calorimeters with the construction and tests (EM parameters only) of a small hadronic prototype module. We plan to request a beam test at either SLAC or FNAL. We will compare the test beam result with Monte Carlo simulations of the prototypes.

In phase two of the R&D project (assuming promising results from phase one) we will propose to extend the size of the hadronic prototype and test it with beams of hadrons and electrons to measure basic parameters of this detector such as energy and position resolutions, e/h rejection power etc. We will also investigate readout methods based on APDs and/or SiPMs and compare them with the PMT readout.

Budget

Based on quotes received so far, and using our prior experience, we have estimated the cost of the R&D for a non-projective “spacordion” type electromagnetic calorimeter and a small prototype for the SPACAL type calorimeter in Table 3. This cost will cover most of our efforts in the phase one of the proposed R&D project.

Tungsten powder, BCF12 scintillating fibers, epoxy and misc. mechanical components for 4x4 matrix “spacordion” EMC prototype.	\$10k
Tungsten powder, BCF20 scintillating fibers, epoxy and misc. mechanical components for 4x4 matrix SPACAL type combined EM+HAD small prototype.	\$30k
Upgrade for DAQ and test run equipment (electronics, test run counters, sc. hodoscopes, cables etc.) (includes 26% overhead)	\$15k
Machine Shop	\$20k
Undergrad/Grad students labor (includes 26% overhead)	\$10k
Shipping (includes 26% overhead)	\$10k
Travel (5 people, 1 x 3 weeks) (includes 26% overhead)	\$15k
Total direct cost	\$97k
Total indirect cost	\$13k
Anticipated BNL contract overhead	\$17.46k
Total	\$127.46k

Table 3. Cost breakdown for phase one of the proposed R&D project.

REFERENCES:

1. Scintillating-fiber calorimetry, M. Livan, V. Vercesi, R. Wigmans . CERN Yellow Report, CERN-95-02
2. The DREAM Project –Results and plans, R. Wigmans, NIM A 572 (2007) 215-217

3. Performance of an Electromagnetic Lead/Scintillating-Fiber Calorimeter for the H1 Detector. H1 SPACAL GROU, DESY Red Report 95-165, NIM A374 (1996) 149-156
4. G. Drews et al., NIM A290 (1990) 335
5. E. Bernardi et al., NIM A262 (1987) 229
6. D. Acosta et al., NIM A308 (1991) 481
7. Quartz Fibers and the Prospect for Hadron Calorimetry at the 1% resolution level, R. Wigmans, Proceedings of the 7th International Conference on Calorimetry in HEP, Tucson 1997.
8. R. Wigmans, Calorimetry, Energy Measurement in Particle Physics, International Series of Monographs on Physics, Vol. 107, Oxford University Press, Oxford 2000.
9. R. Wigmans, NIM A259 (1987) 389
10. D. Acosta et al., NIM B62 (1991) 116-132
11. R. Wigmans, NIM A494 (2002) 277-287
12. N. Akchurin, et al, NIM A 598 (2009) 710-721
13. N. Akchurin, et al, NIM A 408 (1998) 380
14. TESLA Technical Design Report, Report DESY 2001-011, DESY, Hamburg, Germany, 2001
15. D. Acosta, et al., NIM A305 (1991) 55
16. 4th Letter of Intent. <http://www.4thconcept.org/4LoI.pdf>
17. A. C. Benvenuti et al., NIM A 461(2001) 373-375
18. C. Leroy and P. G. Rancoita, Rep. Prog. Phys. 63 (2000) 505-606